ЕЛЕКТРОДИНАМІКА. ПРИСТРОЇ НВЧ ДІАПАЗОНУ. АНТЕННА ТЕХНІКА

UDC 621.396

EIGENMODES ANALYSIS OF SECTORAL COAXIAL RIDGED WAVEGUIDES BY TRANSVERSE FIELD-MATCHING TECHNIQUE. PART 2. NUMERICAL RESULTS

F. F. Dubrovka, Doctor of Science (Technics), Professor
S. I. Piltyay, Postgraduate Student
National Technical University of Ukraine «Kyiv Polytechnic Institute», Kyiv, Ukraine

АНАЛІЗ ВЛАСНИХ ХВИЛЬ СЕКТОРНИХ КОАКСІАЛЬНИХ РЕБРИСТИХ ХВИЛЕВОДІВ МЕТОДОМ УЗГОДЖЕННЯ ПОЛІВ ЧАСТКОВИХ ОБЛАСТЕЙ. ЧАСТИНА 2. ЧИСЕЛЬНІ РЕЗУЛЬТАТИ.

Дубровка Ф. Ф., д.т.н, професор; Пільтяй С. І., аспірант
Національний технічний університет України «Київський політехнічний інститут», м. Київ, Україна

Introduction

For development of devices based on ridged structures one needs to know modal characteristics of ridged waveguides, namely, modes cutoff frequencies and field distributions. The characteristics of ridged waveguides eigenmodes for rectangular cross-section have been analyzed in [1, 2], for square — in [3], for circular — in [1], for elliptical — in [4], for rectangular coaxial — in [5]. In [6] authors of this paper have solved the electrodynamics boundary problem for the sectoral coaxial ridged waveguides (SCRW) using transverse field-matching technique (TFMT).

In this paper we present results of numerical research of the eigenmodes in SCRW using TFMT. Results for cutoff wave numbers are compared with those obtained in [7, 8] by integral equation technique (IET).

Configurations of hollow SCRW under study and denotations of their cross sectional dimensions are shown in Fig. 1, namely the SCRW with a ridge on the inner wall is shown in Fig. 1*a*, and the SCRW with a ridge on the outer wall is shown in Fig. 1*b* (hereinafter referred to as subscripts "in" and "out" respectively). Only the modes, for which the SCRW symmetry plane is a magnetic wall, are investigated.

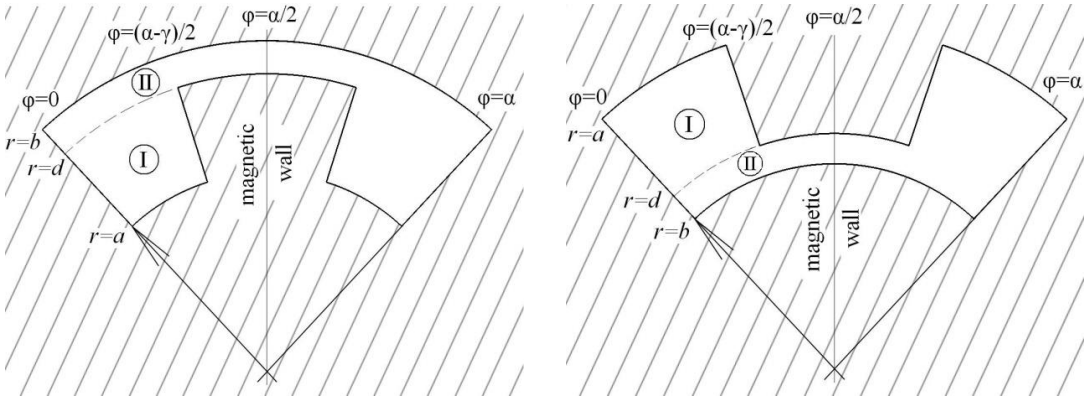

Fig. 1. SCRW configurations and denotations of their cross sectional dimensions

Cutoff wave numbers

In this section we investigate cutoff wave numbers of several modes of both SCRW configurations (Fig. 1) with fixed flare angle $\alpha = 86°$ at the resizing of relative ridge height h for different angular ridge sizes γ and inner-to-outer radii ratios. The results of calculations of cutoff wave numbers multiplied by the outer radius of the SCRW with a ridge on inner ($k_{c\,in}b$) or outer ($k_{c\,out}a$) wall obtained by TFMT and IET [7, 8], which are implemented in our own software, are shown in Fig. 2–7. The deviation between the results for cutoff wave numbers obtained by these two techniques is less than 0.5 %.

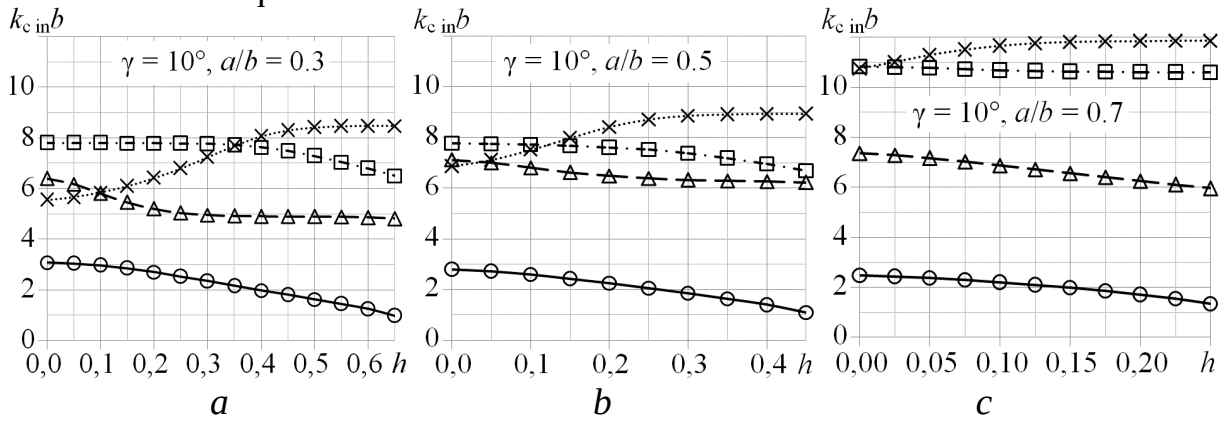

Fig. 2. Cutoff wave numbers ($k_{c\,in}b$) of the SCRW with a ridge on inner wall

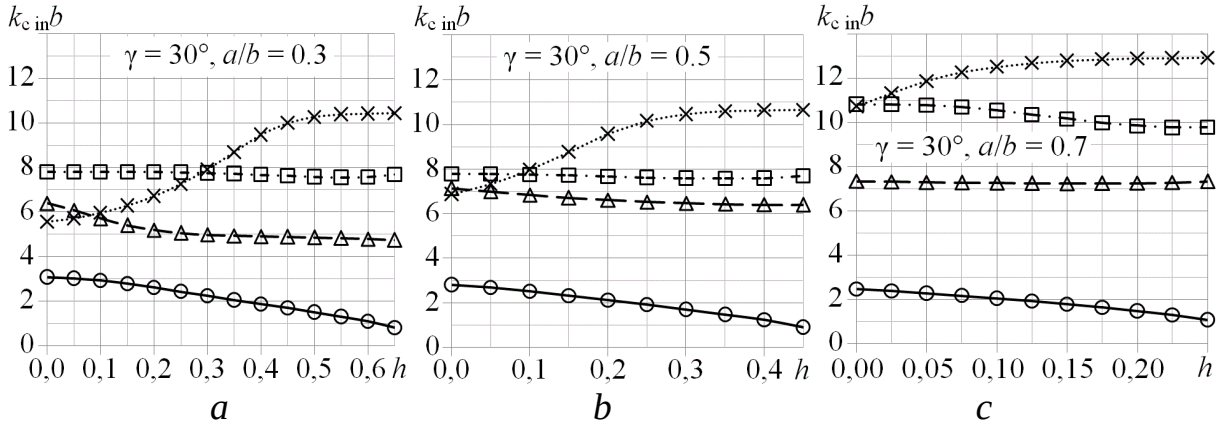

Fig. 3. Cutoff wave numbers ($k_{c\,in}b$) of the SCRW with a ridge on inner wall

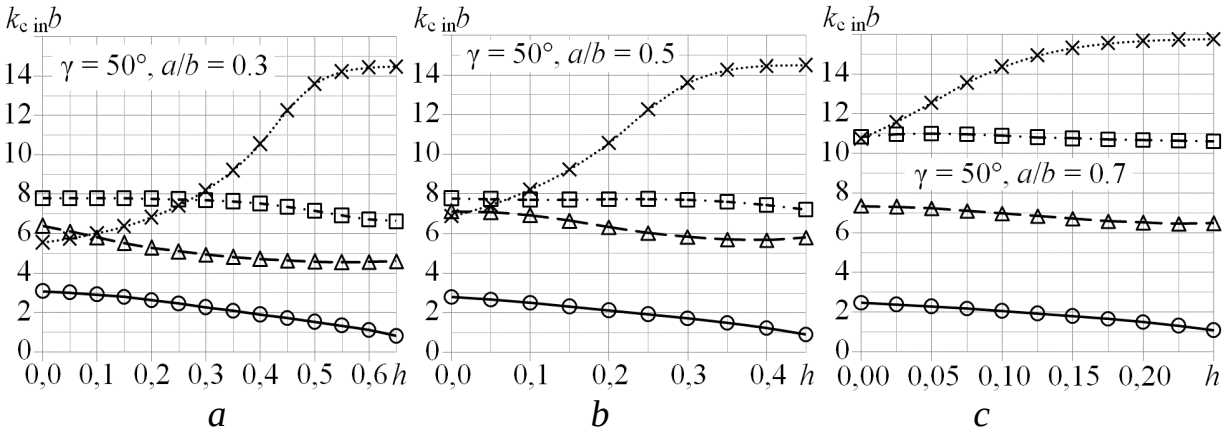

Fig. 4. Cutoff wave numbers ($k_{c\,in}b$) of the SCRW with a ridge on inner wall

In Fig. 2–7 the results obtained by IET are shown by lines, and the ones obtained using TFMT — by symbols. The results for the first TE mode are shown by solid lines and circles, for the second TE mode — by dashed lines and triangles, for the third TE mode — by dash-dotted lines and squares, for the first TM mode — by dotted lines and diagonal crosses.

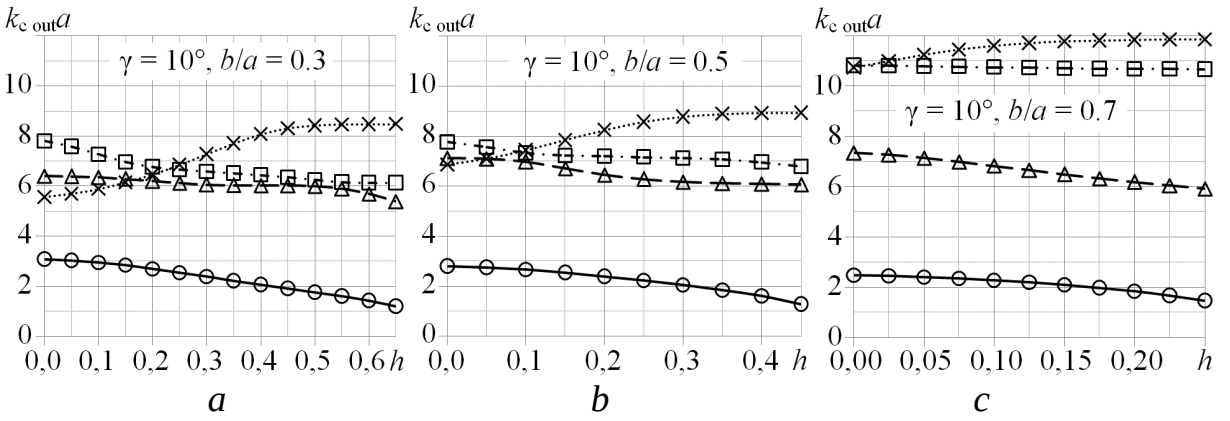

Fig. 5. Cutoff wave numbers ($k_{c\,out}a$) of the SCRW with a ridge on outer wall

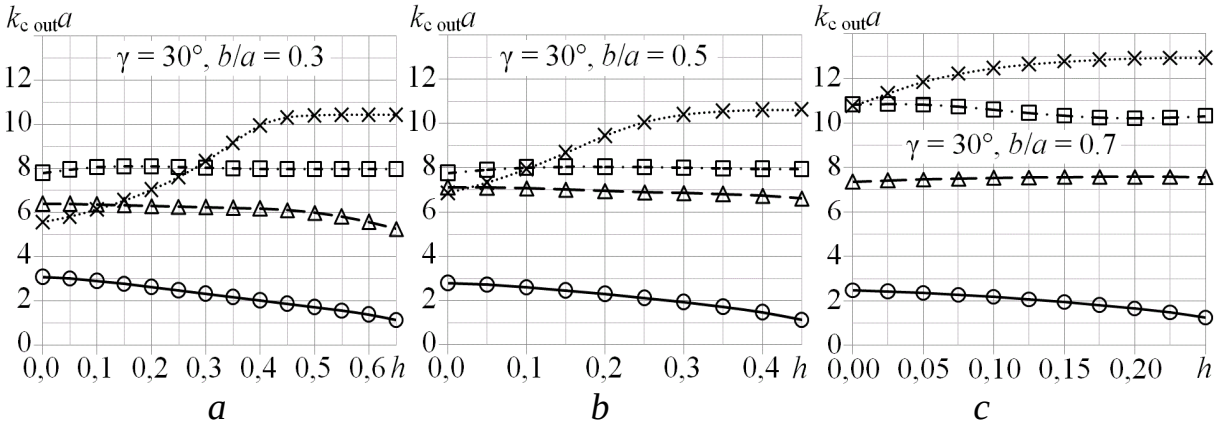

Fig. 6. Cutoff wave numbers ($k_{c\,out}a$) of the SCRW with a ridge on outer wall

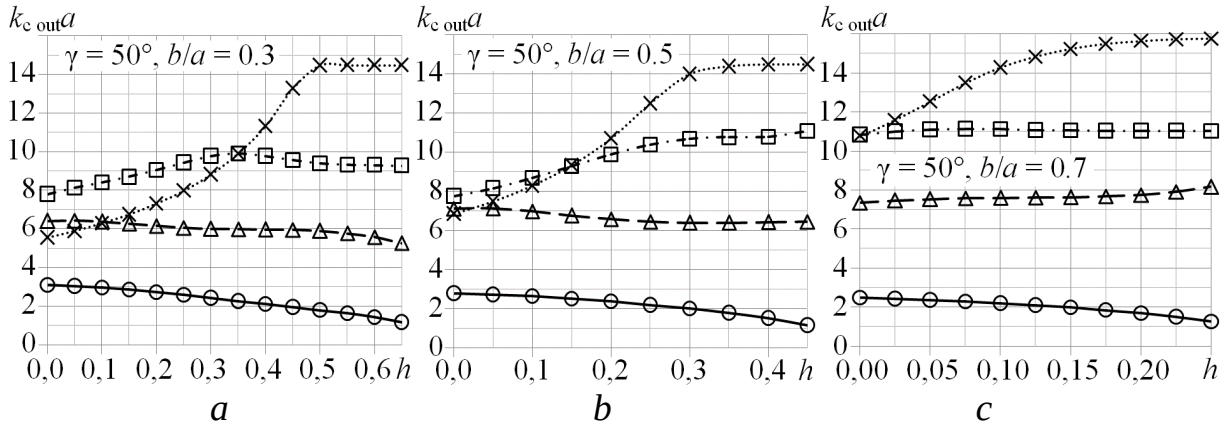

Fig. 7. Cutoff wave numbers ($k_{c\,out}a$) of the SCRW with a ridge on outer wall

The results for the SCRW with a ridge on inner wall are shown in Fig. 2–4, and for SCRW with a ridge on an outer wall — in Fig. 5–7. In Fig. 2–7 the dependences of cutoff wave numbers on relative height $h = (d–a)/b$ are shown at $\gamma = 10, 30, 50°$ and $a/b = 0.3; 0.5; 0.7$ (Fig. 2–4) and $h = (a–d)/a$ at $\gamma = 10, 30, 50°$ and $b/a = 0.3; 0.5; 0.7$ (Fig. 5–7) respectively.

As one can see in Fig. 2–7 at any geometrical configurations of SCRW the fundamental mode is TE one. At inner-to-outer radii ratio less than 0.5 and low ridge ($(d–a)/b \le 0.05$ for the SCRW with a ridge on inner wall or $(a–d)/a \le 0.05$ for the SCRW with a ridge on outer wall) the second mode is TM one. Increasing of the ridge height or inner-to-outer radii ratio results in the second mode becomes TE one. The SCRW with relatively high ridges are mostly used in practice, thus single-mode operation frequency band of the SCRW is determined by cutoff frequencies of the two lower TE modes.

Solutions convergence for electric field components distributions

Let us carry out convergence analysis of electric field components distributions depending on the number of partial modes *M*. The calculations have been performed for the fundamental TE mode in both SCRW configurations (Fig. 1). For the SCRW with a ridge on inner wall we set dimensions ratios and angles as follows: $\alpha = 86°$, $\gamma = 30°$, $a/b = 0.5$, $(d–a)/b = 0.4$, and for the SCRW with a ridge on outer wall – as follows: $\alpha = 86°$, $\gamma = 30°$, $b/a = 0.5$, $(a–d)/a = 0.4$.

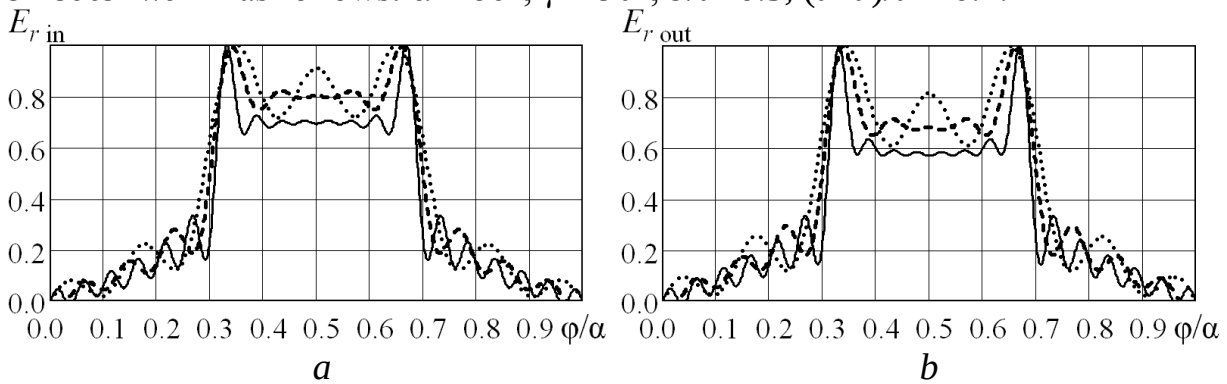

Fig. 8. Fundamental TE mode electric field radial component distribution (parameter is a number of partial modes *M*)

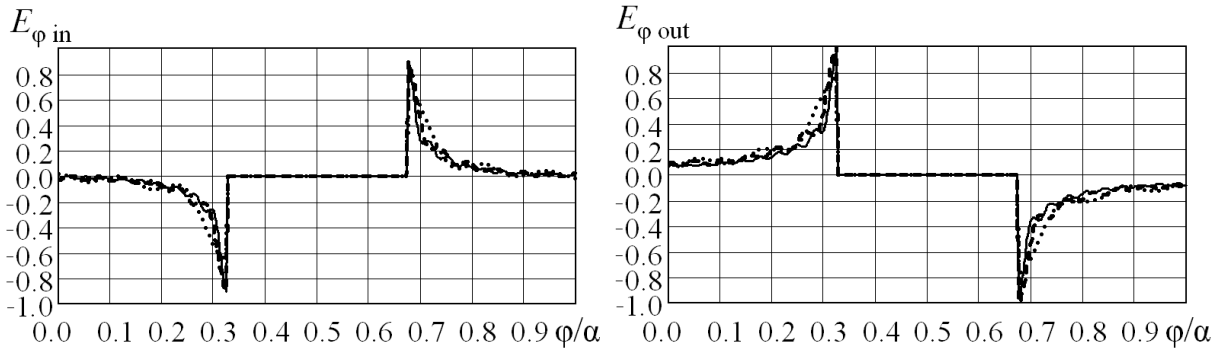

Fig. 9. Fundamental TE mode electric field azimuthal component distribution (parameter is a number of partial modes *M*)

The electric field radial component E_r computed at the interface between the regions I and II is shown in Fig. 8, and the azimuthal one E_φ — in Fig. 9. In the both figures the results obtained utilizing 10, 20 and 30 partial modes are shown by dotted, dashed and solid lines respectively. As one can see in Fig. 8, 9 the electric field distributions peaks become sharper as the number of partial modes M increases. Besides, level of electric field radial component in the gap between the ridge and the cylindrical wall decreases and its distribution in the gap becomes more uniform (Fig. 8). The distributions obtained by TFMT at the utilization of 30 partial modes are in good agreement with those obtained by IET with correct singular field behavior at the ridge [8]. Consequently, for the correct calculation of the SCRW field distributions by TFMT one should utilize not less than 30 partial modes.

Electric field components distributions

In this section we investigate electric field distributions in the SCRW of both configurations with the same geometry which was set in the convergence analysis of cutoff wave numbers and electric field components distributions. In Fig. 10–18 electric field components distributions normalized to the maximal values are shown for three lower TE modes, and in Fig. 19–21 — for the first TM mode. Electric field components distributions for the SCRW with the ridge on inner wall are shown in Fig. 10*a*–21*a*, for the SCRW with the ridge on outer wall — in Fig. 10*b*–21*b*.

The radial components of electric field E_r are shown in Fig. 10, 13, 16, 19, and the azimuthal ones E_φ — in Fig. 11, 14, 17, 20. In Fig. 10, 11, 13, 14, 16, 17, 19, 20 field distributions at cylindrical surface with the radius $(a+b)/2$, that corresponds to the middle of the SCRW lateral regions, are shown by dashed line, at the surface with the radius d, that corresponds to the interface between the regions I and II, — by solid line, at the surface with the radius $(b+d)/2$, that corresponds to the middle of the gap between the ridge and the cylindrical wall, — by dotted line.

All electric field components distributions computed by TFMT and shown in Fig. 10–21 are in good agreement with those obtained by IET with correct taking into account singular field behavior at the ridge [8]. This confirms the correctness of the results obtained.

Having compared Fig. 2–4 with Fig. 5–7 one can see, that cutoff wave numbers of the first TE and TM modes depend on relative ridge height for both SCRW configurations almost identically. Cutoff wave number and cutoff frequency of the SCRW fundamental TE mode decreases monotonically as the ridge height increases. At the same time electric and magnetic fields of the fundamental mode are concentrated near the edge of the ridge and in the gap between the ridge and the cylindrical wall of the SCRW (Fig. 10–12).

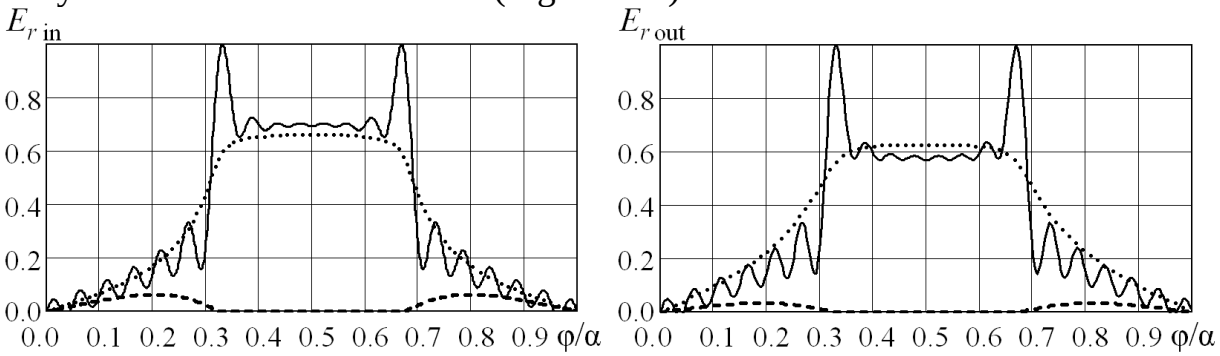

a *b*

Fig. 10. Electric field radial component of the fundamental TE mode

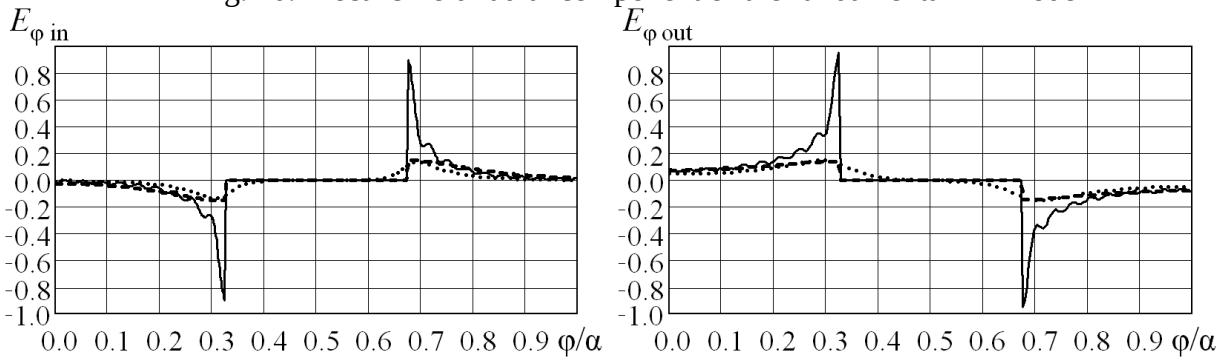

a *b*

Fig. 11. Electric field azimuthal component of the fundamental TE mode

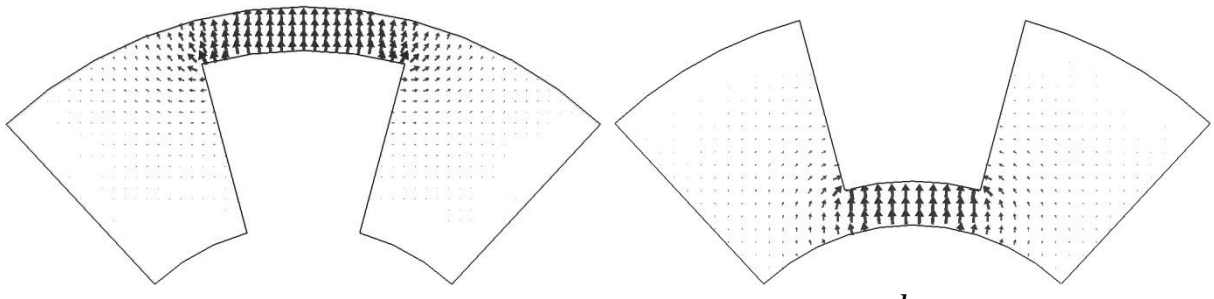

a *b*

Fig. 12. Vector electric field distribution of the fundamental TE mode

As one can see in Fig. 10 electric field radial component of the fundamental mode at the ridge edges is in-phase with the field in the gap between the ridge and

the cylindrical wall. It can be inferred from Fig. 10, 11 that the maximal values of radial and azimuthal components of fundamental mode electric field are obtained near the ridge edges. Moving away from the ridge edge in any direction the azimuthal component of electric field decreases drastically and it almost completely centred in the vicinity of the ridge edge.

It is seen in Fig. 13 and 16 that the electric field radial component of two higher TE modes at ridge edges is in-phase with the field in the gap between the ridge and the cylindrical wall for the SCRW with the ridge on outer wall and is anti-phase with it for the SCRW with the ridge on inner wall.

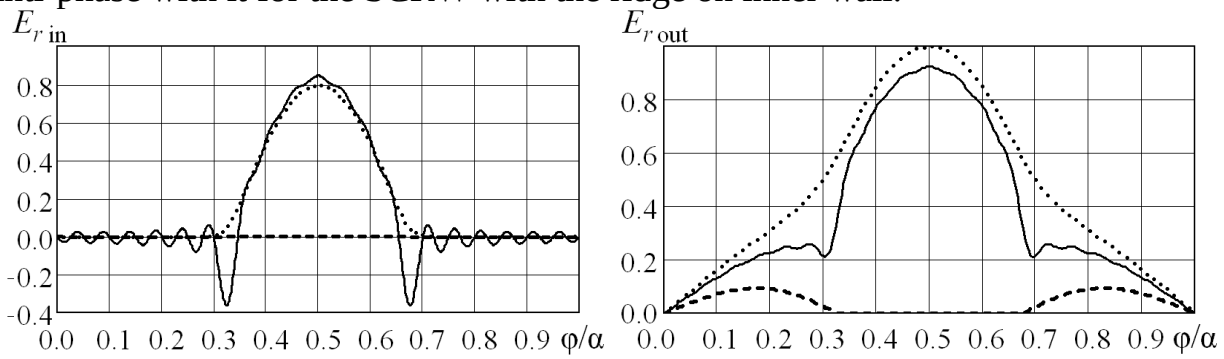

Fig. 13. Electric field radial component of the second TE mode

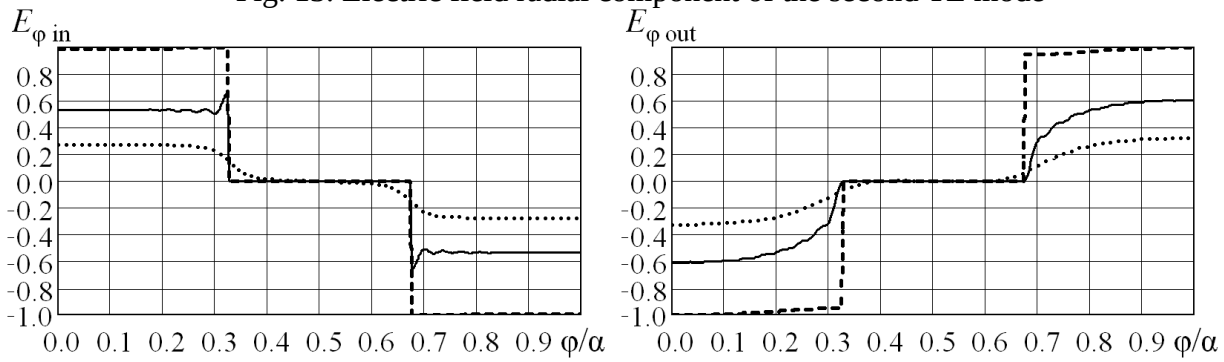

Fig. 14. Electric field azimuthal component of the second TE mode

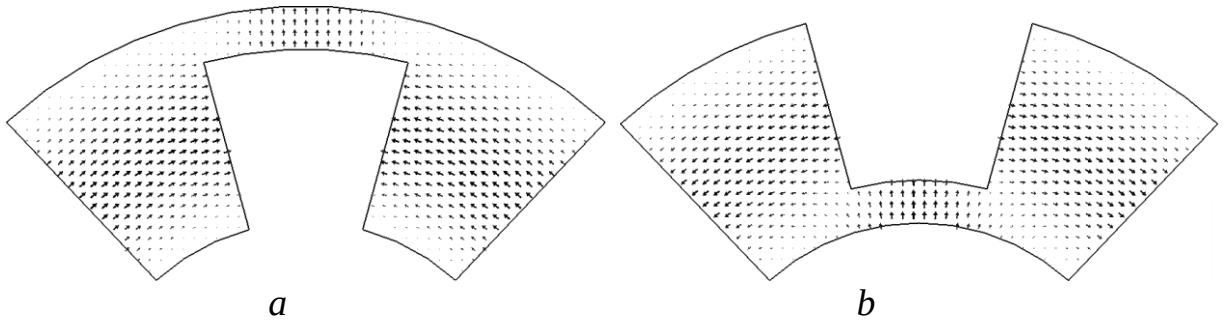

Fig. 15. Vector electric field distribution of the second TE mode

As one can see in Fig. 13–15 the electric field radial component for the second TE mode is almost completely concentrated in the gap between the ridge and the cylindrical wall, and the azimuthal one — in the lateral regions of the SCRW, where its angular distribution is almost uniform.

It can be concluded from Fig. 19–21 that at the relatively high ridge the electric field components of the first TM mode are concentrated in the lateral regions of the SCRW. This is induced by the fact, that the longitudinal component of electric field is tangential to the surface of the ridge and to the cylindrical wall of the SCRW. At the narrow gap this component is extruded from it. The transversal components of electric and magnetic fields of TM modes are determined by the longitudinal component of electric field. That's why electric and magnetic fields of lower TM modes are almost absent in the narrow gap.

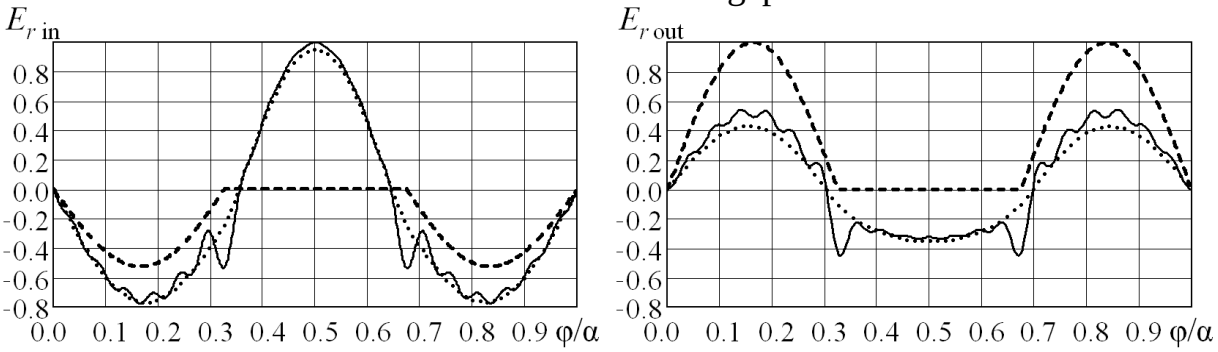

a *b*

Fig. 16. Electric field radial component of the third TE mode

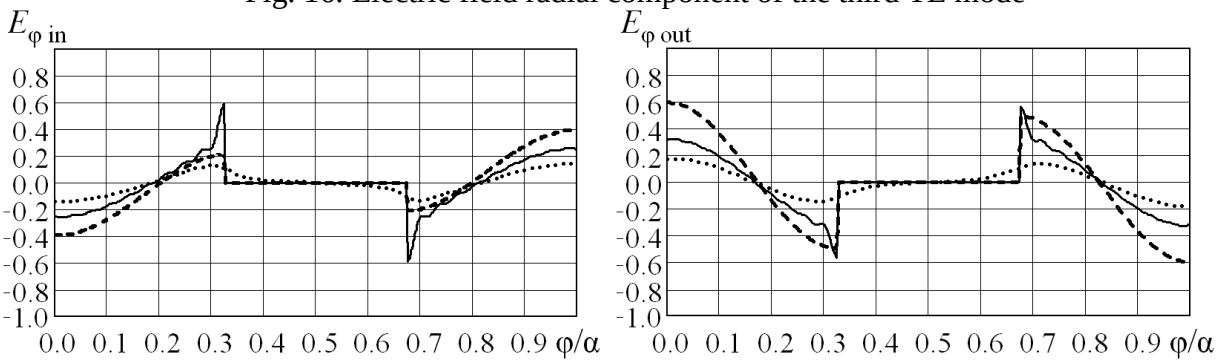

a *b*

Fig. 17. Electric field azimuthal component of the third TE mode

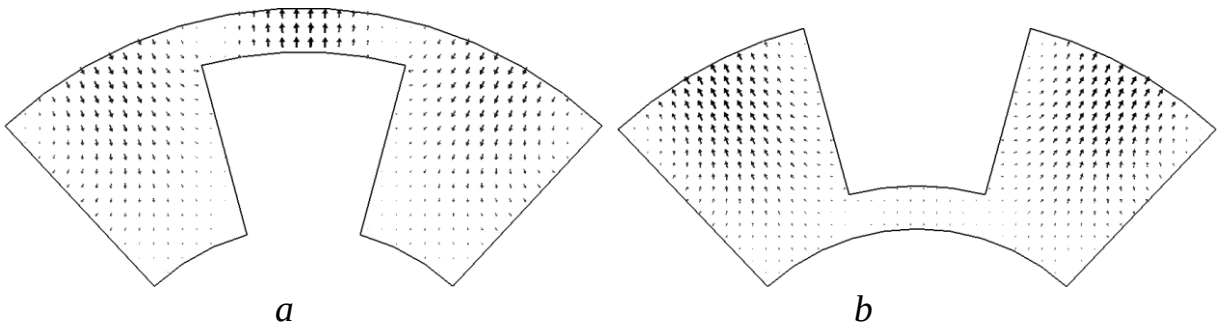

a *b*

Fig. 18. Vector electric field distribution of the third TE mode

Conclusions

Parametric study of cutoff wave numbers and numerical investigation of electric field components distributions of first four modes of the SCRW with the ridge on inner or outer wall have been carried out. It has been shown that for the correct calculation of SCRW field distributions by TFMT one should utilize more

than 30 partial modes. In this case electric field components of the fundamental TE mode are concentrated near the edge of the ridge and in the gap between the ridge and the cylindrical wall. Maximal values of electric field radial and azimuthal components of this mode take place near the ridge edges. Moving away from the ridge's edge in any direction the azimuthal component of electric field decreases drastically and it almost completely centred in the vicinity of the ridge edge. These results completely confirm singular behavior of the electric field components at an edge.

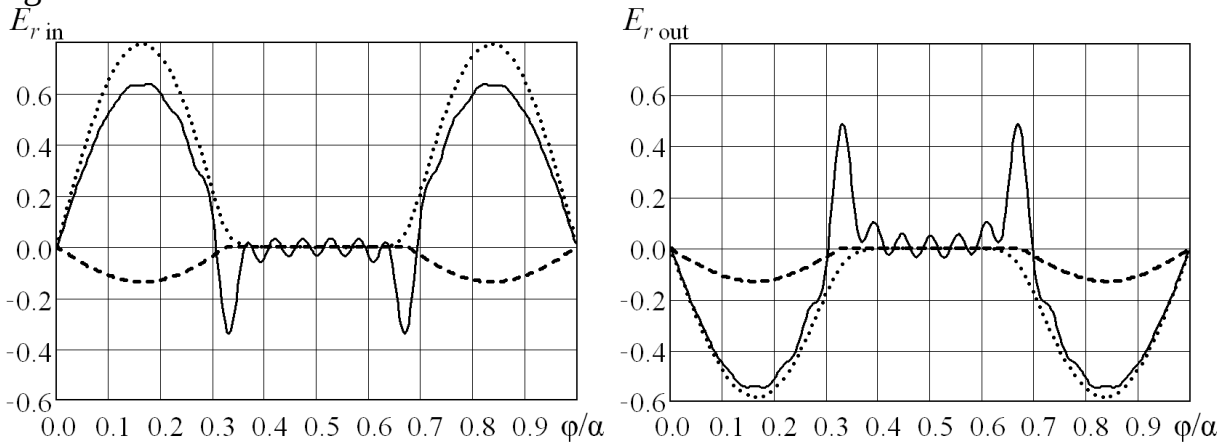

a *b*

Fig. 19. Electric field radial component of the first TM mode

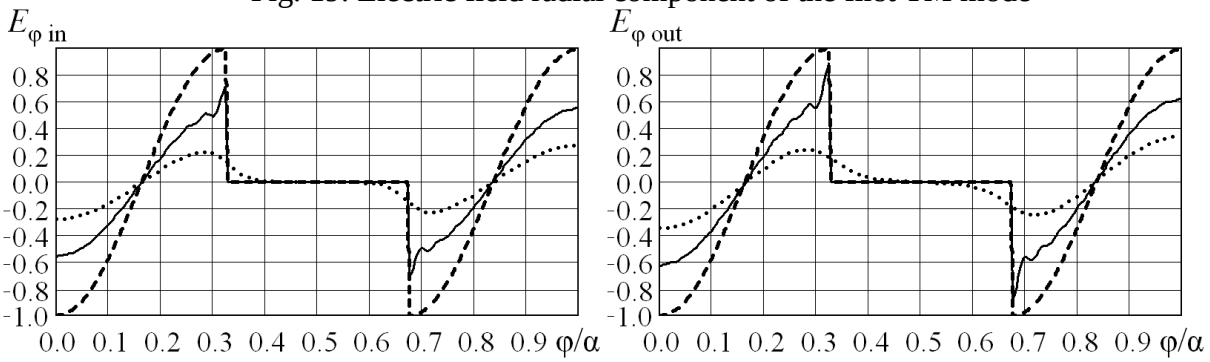

a *b*

Fig. 20. Electric field azimuthal component of the first TM mode

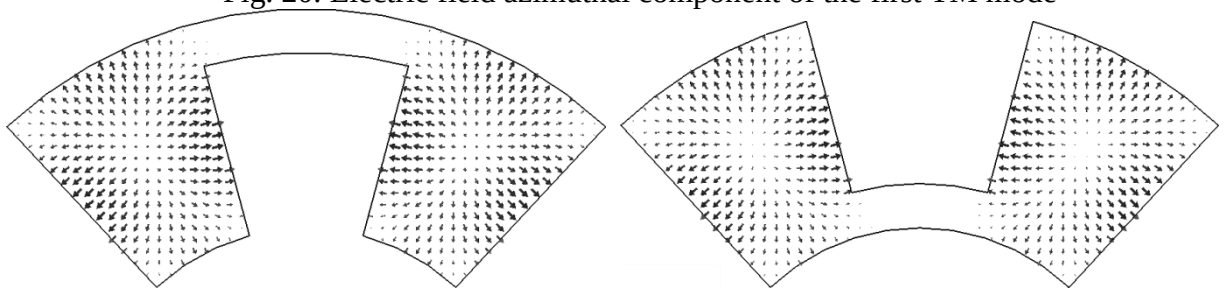

a *b*

Fig. 21. Vector electric field distribution of the first TM mode

Electric field radial component for the second TE mode is almost completely concentrated in the gap between the ridge and the cylindrical wall, and the azimuthal one — in the lateral regions of the SCRW, where its angular distribution

is almost uniform. At relatively high ridge of the SCRW the fields of lower TM mode are almost absent in the gap between the ridge and the cylindrical wall, they are concentrated in the lateral regions of the SCRW.

All electric field components distributions computed by TFMT are in good agreement with those obtained by IET with correct taking into account of the singular field behavior at the ridge [8].

References

1. Rong Y., Zaki K. A. (2000) Characteristics of generalized rectangular and circular ridge waveguides // *IEEE Trans. Microwave Theory Tech*., vol. 48, no 2, pp. 258–265. doi: 10.1109/22.821772

2. Jarvis D. A., Rao T. C. (2000) Design of double-ridged rectangular waveguide of arbitrary aspect ratio and ridge height // *IEE Proc. AP*. vol. 147, no 1, pp. 31–34. doi: 10.1049/ip-map:20000013

3. Tang Y., Zhao J., Wu W. (2006) Analysis of quadruple-ridged square waveguide by multilayer perceptron neural network model // *Asia-Pacific Microwave Conference (APMC 2006)*, Yokohama, Japan, pp. 1912–1918. doi: 10.1109/APMC.2006.4429782

4. Xu J., Wang W., Gong Y., Wei Y. (2006) Analysis of elliptical ridged waveguide // *Joint 31st International Conference on Infrared Millimeter Waves and 14th International Conference on Teraherz Electronics (IRMMW-THz 2006)*, Shanghai, China, p. 265. doi: 10.1109/ICIMW.2006.368473

5. Ruiz-Bernal M. A., Valverde-Navarro M., Goussetis G., Gomez-Tornero J.-L., Feresidis A. P. (2006) Higher order modes of the ridged coaxial waveguide // *36th European Microwave Conference*, Manchester, UK, pp. 1221-1224. doi: 10.1109/EUMC.2006.281197

6. Dubrovka F. F., Piltyay S. I. (2013) Eigenmodes analysis of sectoral coaxial ridged waveguides by transverse field-matching technique. Part 1. Theory // *Bulletin of NTUU "KPI". Series Radiotechnique. Radioapparatus Building*. no. 54, pp. 13–23. Available at: http://radap.kpi.ua/index.php/radiotechnique/article/view/657

7. Dubrovka F. F., Piltyay S. I. (2012) Electrodynamics boundary problem solution for sectoral coaxial ridged waveguides by integral equation technique // *Radioelectronics and Communications Systems*. vol. 55, no 5, pp. 191–203. doi: 10.3103/S0735272712050019

8. Dubrovka F. F., Piltyay S. I. (2012) Eigenmodes of sectoral coaxial ridged waveguides // *Radioelectronics and Communications Systems*. vol. 55, no 6, pp. 239-247. doi: 10.3103/S0735272712060015

Дубровка Ф. Ф., Пільтяй С. І. ***Аналіз власних хвиль секторних коаксіальних ребристих хвилеводів методом узгодження полів часткових областей. Частина 2. Результати.*** *Методом узгодження полів часткових областей розв'язано крайову задачу електродинаміки для власних хвиль секторних коаксіальних одноребернх хвилеводів. Установлено, що для точного розрахунку розподілів полів методом узгодження полів часткових областей потрібно використовувати більше ніж 30 парціальних мод. Представлено розподіли електричного поля перших чотирьох мод секторних коаксіальних ребристих хвилеводів із ребром на внутрішній і зовнішній стінці.*

Ключові слова: *крайова задача електродинаміки, секторний коаксіальний ребристий хвилевід, метод узгодження полів часткових областей, власні хвилі типу ТЕ, власні хвилі типу ТМ, розподіл поля.*

Дубровка Ф. Ф., Пильтяй С. И. ***Анализ собственных волн секторных коаксиальных ребристых волноводов методом согласования полей частичных областей. Часть 2. Результаты.*** *Методом согласования полей частичных областей решена краевая задача электродинамики для собственных волн секторных коаксиальных однореберных волноводов. Установлено, что для точного расчета распределений полей методом согласования полей частичных областей необходимо использовать больше чем 30 парциальных мод. Представлены распределения электрического поля первых четырех мод секторных коаксиальных ребристых волноводов с ребром на внутренней и внешней стенке.*

Ключевые слова: *краевая задача электродинамики, секторный коаксиальный ребристый волновод, метод согласования полей частичных областей, собственные волны типа ТЕ, собственные волны типа ТМ, распределение поля.*

Dubrovka F. F., Piltyay S. I. ***Eigenmodes analysis of sectoral coaxial ridged waveguides by transverse field-matching technique. Part 2. Numerical results.***

Introduction. The goals of the research presented in the paper are defined. The geometrical configurations of sectoral coaxial ridged waveguides are shown.

Cutoff wave numbers. The results of calculations of cutoff wave numbers multiplied by the outer radius of sectoral coaxial ridged waveguide with a ridge on an inner or outer wall obtained by transverse field-matching technique and integral equation technique are shown for the first four modes. The deviation between the results for cutoff wave numbers obtained by these two techniques is less than 0.5 %.

Solutions convergence for electric field components distributions. The convergence analysis of electric field components distributions depending on the amount of partial modes is carried out. It is shown, that for correct calculation of sectoral coaxial ridged waveguides field distributions by transverse field-matching technique one should utilize more than 30 partial modes.

Electric field components distributions. The electric field distributions in sectoral coaxial ridged waveguides of both configurations are investigated for the first four modes. All electric field components distributions computed by transverse field-matching technique are in good agreement with the ones obtained by integral equation technique with correct account of the singular field behavior at the ridge. This confirms the correctness of the results obtained.

Conclusions. General conclusions of the paper are given.

Keywords*: electrodynamics boundary problem, sectoral coaxial ridged waveguide, transverse field-matching technique, TE modes, TM modes, field distribution.*